Economic and technological feasibility of using power-to-hydrogen technology under higher wind penetration in China

Haiyang Lin, Qiuwei Wu, Xinyu Chen, Xi Yang, Xinyang Guo, Jiajun Lv, Tianguang Lu, Shaojie Song, Michael Mcelroy

Economic and technological feasibility of using power-to-hydrogen technology under higher wind penetration in China

Haiyang Lin [a, b], Qiuwei Wu [c], Xinyu Chen [b, d, **], Xi Yang [b, e], Xinyang Guo [d], Jiajun Lv [f], Tianguang Lu [b, g], Shaojie Song [b], Michael McElroy [b, *]

[a] Institute of Thermal Science and Technology, Shandong University, Jinan, 250061, China
[b] John A. Paulson School of Engineering and Applied Sciences, Harvard University, Cambridge, MA, 02138, USA
[c] Center for Electrical Power and Energy (CEE), Department of Electrical Engineering, Technical University of Denmark, Kgs. Lyngby, 2800, Denmark
[d] State Key Laboratory of Advanced Electromagnetic Engineering and Technology, School of Electrical and Electronic Engineering, Huazhong University of Science and Technology, Wuhan, 430074, China
[e] School of Economics and Management, China University of Petroleum Beijing, Beijing, 102249, China
[f] School of Electronics and Information, Xi'an Polytechnic University, China
[g] School of Electrical Engineering, Shandong University, Jinan, 250061, China

a b s t r a c t

Hydrogen can play a key role in facilitating the transition to a future deeply decarbonized energy system and can help accommodate higher penetrations of renewables in the power system. Arguments to justify this conclusion are supported by an analysis based on real-world data from China's Western Inner Mongolia (WIM). The economic feasibility and decarbonization potential of renewable-based hydrogen production are discussed through an integrated power-hydrogen-emission analytical framework. The framework combines a high-resolution wind resource analysis with hourly simulation for the operation of power systems and hydrogen production considering technical and economic specifications on selection of three different types of electrolyzers and two operating modes. The results indicate that using wind power to produce hydrogen could provide a cost-competitive alternative (<2 $kg^{-1}) to WIM's current coal-dominated hydrogen manufacturing system, contributing at the same time to important reductions in wind curtailment and CO_2 emissions. The levelized cost for hydrogen production is projected to decrease in the coming decade consistent with increases in wind power capacity and decreases in capital costs for electrolyzers. Lessons learned from the study can be applied to other regions and countries to explore possibilities for larger scale economically justified and carbon saving hydrogen production with renewables.

1. Introduction

Wind and solar sources have been regarded as the most promising contributors to decarbonizing the energy sector. China, leading in installed capacities of both wind and solar power systems globally, doubled both of these resources between 2016 and 2020 (to about 400 GW in total) [1]. However, effective integration of these variable sources into a relatively inflexible energy system poses a major challenge at high levels of renewable penetration [2]. The importance of flexibility is underappreciated in traditional power system planning. In North China, where the largest onshore wind farms are located, the installed wind capacity reached 59 GW in 2019 [3]. Despite this, coal-fired power plants, which are inflexible compared to gas-fired and hydro power units, dominate the local generation mix. Especially during the heating season, coal-based combined heating and power (CHP) generation systems are often must-run units and their operational flexibility is reduced accordingly [4]. The Chinese national wind power curtailment rate reached as high as 21% in 2016 [5]. The investment in wind power is facing challenges due to this high wind curtailment rate. For instance, the cumulative financial loss due to wind curtailment was over 1.2 billion USD in China over the period 2010e2016 [6].

* Corresponding author.
** Corresponding author. John A. Paulson School of Engineering and Applied Sciences, Harvard University, Cambridge, MA, 02138, USA.
E-mail addresses: xchen2019@hust.edu.cn (X. Chen), mbm@seas.harvard.edu (M. McElroy).

Developing an economically viable strategy to reduce wind curtailment would represent a critical step in realizing a higher penetration of renewables. Apart from conventional strategies to deploy storage options such as pumped hydro and compressed air, power-to-hydrogen (P2H) technology could play a key role in improving the integration of renewables and facilitating the transition to a future deeply decarbonized energy system [7].

Hydrogen has been an important industrial feedstock for decades. The largest shares of hydrogen in China are deployed in the chemical industry for production of ammonia (75.8%) and methanol (10.5%), and for hydrocracking and hydrotreatment in refineries (13.7%) [8]. In high-temperature industries such as iron & steel production, the application of hydrogen is seen as an important prospective way to advance decarbonization [8]. However, over 95% of the current hydrogen production in China is based on fossil fuels [9]. Coal gasification is widely used due to both shortages and high prices of natural gas in China, but the CO_2 emissions associated with production of hydrogen from coal are twice as high as the corresponding source for production from natural gas [10]. Hydrogen from renewables (yielding so-called "green" hydrogen) could replace fossil-fuel-based feedstocks in these CO_2-emission-intensive industrial applications. Green hydrogen could also be injected into natural gas distribution networks, serving to reduce at least part of the demand for carbon-emitting natural gas [11]. When fueled by green hydrogen, fuel cell electric vehicles (FCEVs) could provide a low-carbon mobility option and offer driving experience comparable or even superior to that associated with conventional vehicles [12,13]. Consumption of electricity through electrolysis could help realize a high penetration of renewables in power systems, not only enhancing the overall efficiency of the energy system but providing also a valuable source of carbon-free hydrogen [14]. Electrolytic green hydrogen has so far been regarded as an expensive option mainly because of the relatively high cost of electricity [15]. Regions with rich renewable resources however have significant potential for large scale production of hydrogen at reasonable cost. Specifically, the abundant curtailed renewable power resources and a declining trend in the cost of renewable power production suggest the possibility for a significant change in the cost effectiveness of P2H technologies over the relatively immediate future.

Opportunities for green hydrogen production have received significant attention in recent years. Studies on production methods are assessed primarily based on energy, exergy and average cost [16,17]. Researchers calculated balance-of-system costs for standalone and grid-connected solar-hydrogen production with proton-exchange membrane (PEM) electrolysis systems [18] and took advantage of fluctuations in electricity markets to optimize the net present value of a wind-hydrogen system by selling or converting intermittent wind power [19]. On-site green hydrogen production systems have been introduced for refueling of light-duty vehicles [20] and for support of fuel cell buses [21] depending on availability of power at station sites. Some other green hydrogen systems were designed to realize uninterrupted power supply [22,23], to produce synthetic fuels by capturing CO_2 [24], and to facilitate a clean and reliable power, heat and water nexus [25]. These previous studies focused on off-grid or small-scale systems. They did not consider the dynamic integration of large-scale renewable sources into grid operations to differentiate the temporal variations of available and curtailed wind power, as well as the power purchasing strategies for green hydrogen production facilities. These factors are critical for investigating the green hydrogen production volume and associated costs. A number of studies have considered grid operation together with constrained transmission for hydrogen production [26,27]. However, they involved only simplified formulations assuming generally constant power consumption for associated P2H systems. Integrated with renewable energy, an electrolyzer operates with a variable load and faces frequent start-ups and shutdowns [28]. Additional energy is also required for sub-units to maintain the balance of plant [29,30]. These considerations of partial load operation, auxiliary consumption and lifetime degradation are essential inputs to determining the cost-effectiveness of different P2H technologies with renewables, but have been largely ignored in previous studies. Given the dynamic operational schemes for an integrated power system under higher wind penetration and diverse characteristics for electrolysis systems with variable loads, the technical and economic feasibility for deployment of different types of large-scale P2H technologies in China is as yet unclear.

The cost of hydrogen production is sensitive to many factors including plant capacity, vintage, feedstock, production method, and location. In China, the average costs for hydrogen production via coal gasification are 1.48 $/kg [31] and 2.23 $/kg [32] without and with carbon capture and storage (CCS), respectively. As a gas importer, China has to contend with a relatively high natural gas price, and that makes for higher hydrogen production costs for steam-methane reforming: 1.92 and 2.46 $/kg without and with CCS [31,32]. The P2H technologies have been held back due to lack of technical and economic feasibility, with high cost of 3.34e17.3 $/kg [33]. Studies have concluded that green hydrogen was not yet cost competitive for industrial-scale supply compared with traditional sources from fossil fuels [18,19]. Similar conclusions were drawn in Ref. [34], where the levelized cost of hydrogen (LCOH) was minimized in the planning of an integrated energy system. Different from previous studies, we argue here that the current supply of abundant low-price electricity is changing the cost effectiveness of green hydrogen production, considering the current high-level penetration of wind power and the possibility of offsetting revenues from sales for example of related sources of oxygen.

In this paper, we estimate the technical and economic feasibility of using P2H technologies with wind power in China. The targeted area is Western Inner Mongolia (WIM), which hosts China's largest installation of wind farms suffering at the same time from significant wind curtailment. The overall objective is to take advantage of the wind energy in WIM to produce carbon-free hydrogen to meet the regional industrial demand at a cost lower than the marginal cost for fossil fuel-based hydrogen production. Hourly simulations of the power system are conducted in an integrated power and heat optimization (IPHO) model to estimate on-grid additions of wind power as well as its curtailment, inputted then into a novel electrolysis hydrogen production optimization (EHPO) model to minimize the LCOH or alternatively to maximize the overall hydrogen output subject to a specified limitation on cost. The range limitation, efficiency variation, unit boot order and additional energy consumption in auxiliary components of electrolysis processes are considered in the EHPO along with two operational modes: one where we only use curtailed wind power; the other where we consider electricity both from curtailed and additional on-grid sources of wind energy. The year 2030 is selected to explore how the cost and output for hydrogen production could be impacted by future advances in electrolysis technologies combined with increased investments in wind. Since wind power is the only source considered here for electrolysis, the decarbonization effect on the hydrogen-consuming sectors is evaluated according to the annual hydrogen demand and the production scale of carbon-free hydrogen in WIM.

The main contributions of this study are as follows. First, the paper reports an integrated power-hydrogen-emission analytical framework to analyze the hydrogen production from wind power in China. Second, a dynamic integration of large-scale renewable sources into grid operations is considered differentiating patterns

and potential roles for curtailed and grid-supplied wind power. Further, diverse characteristics for electrolysis systems operating with variable loads are formulated in a system optimization model to investigate technical and economic feasibility. The improved dynamic integrated formulation and lessons learned can be applied to other regions/countries to explore possibilities for larger scale economically justified and carbon saving hydrogen production with renewables.

2. Methodology

The overview of the analytical framework of this study is illustrated in Fig. 1. The procedure combines a high-resolution wind resource analysis with hourly simulation for the operation of power systems together with potential hydrogen production. The wind power simulation under high penetration of renewables is conducted at an hourly resolution over the course of a year, employing high-resolution wind speed data derived from a NASA meteorological database. The hourly wind power data are incorporated then in an Integrated Power and Heat Optimization (IPHO) simulation. The analysis accounts for simulation of the hourly power output from each individual generator in WIM as well as for projections on an hourly basis for wind power that would need to be curtailed in the absence of the proposed investments in electrolysis-based production of hydrogen. The information is fed then into the electrolysis hydrogen production optimization (EHPO) model, considering technical and economic specifications on selection of three different types of electrolyzers and two operating modes. Levelized costs or output amounts of product hydrogen are optimized then depending on the type of technology and operation mode adopted for electrolysis.

The implications in terms of system capacities and operational modes for different electrolysis technologies with respect to both quantities and costs for production of hydrogen with wind power in WIM are explored based on real data and rigorous operational simulations. The electricity/heat demands in 2030 are scaled upward with temporal patterns (hourly variations) similar to 2018 allowing in the IPHO simulation for increasing investments in wind, for projected expansions in ultra-high voltage transmission systems, and for anticipated reductions in costs and improvements in the efficiency of electrolysis technologies.

2.1. IPHO model for the optimized simulation

As nearly half of the thermal units in the studied area are coal-based CHP plants, we employ a high-resolution integrated energy system simulation platform, the IPHO model [35]. The IPHO model is a mixed-integer linear programing (MILP) simulator describing the joint operational characteristics of centralized power and district heating systems. Based on the unit commitment model of conventional power system, the reserve requirement, inter-regional transmission constraint and multiple heating zone configurations are considered. With different levels of wind power integration, the model balances power supply for local and inter-regional networks and balances heating supply in the selected districts on an hourly basis.

The framework of the IPHO model is given in Fig. 2. The inputs include hourly power and heating demands, topology of power networks and configuration in multiple heating districts. The outputs include hourly wind power integration and curtailment, hourly fuel use, energy output and corresponding emissions for individual units.

2.2. Western Inner Mongolia energy systems

The analysis is based on the regional energy system in Western Inner Mongolia (WIM). The WIM area has one of the largest wind bases in China. In this area, the generation mix is mainly constituted by coal-based thermal power and CHP units. The total installed capacity and average fuel use for different units are listed in Table 1.

The generation structure in the WIM region generally represents the typical condition for northern China, where over 50% of the country's onshore wind capacity has been located [36,37]. The capacity expansion of the power system from 2018 to 2030 is estimated taking account of energy demand growth under system investment constraints [38].

2.2.1. Hourly power, heat demand and wind production

Total consumption of electricity in WIM is projected to grow from 232 TWh in 2018 to 430 TWh in 2030 assuming a growth rate consistent with the projected regional power generation expansion [44]. The hourly load profile in 2030 is assumed to follow the same

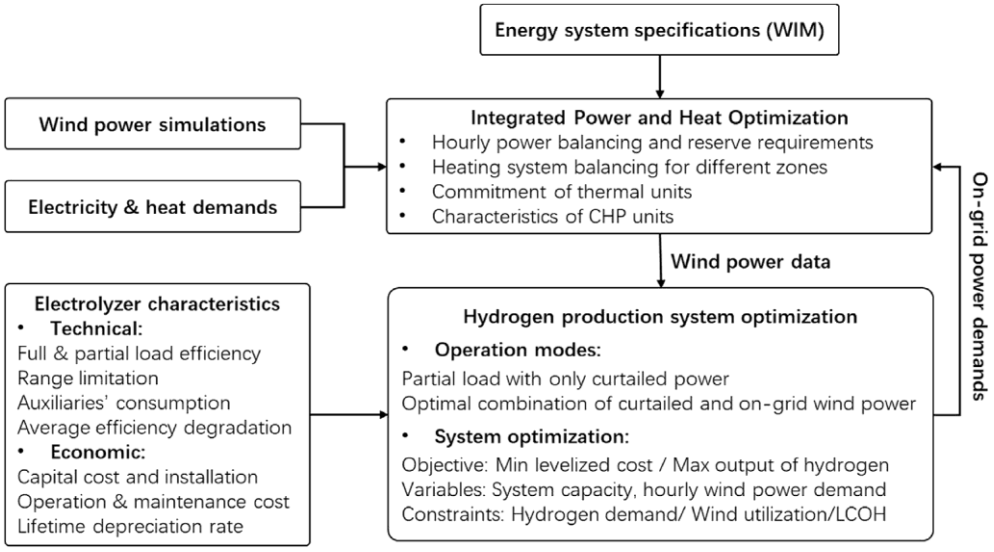

Fig. 1. Analytical framework of hydrogen production simulations.

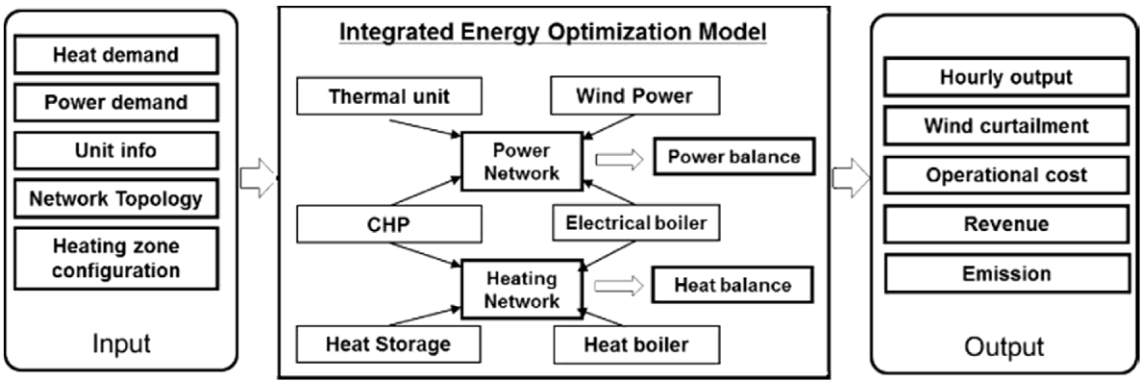

Fig. 2. Modeling framework for IPHO, adapted from Ref. [35].

Table 1
Generation structure in WIM area in 2018.

Type	Total capacity (GW) [39e42]	Average Fuel Use (g/kWh)[a,b] [35,43]
Thermal (Coal)	31	303
Thermal (Gas)	0.3	351
CHP-coal	21.5	311
CHP-gas	/	351
Solar	7.5	/
Wind	18.2	/
Hydro	2	/
Pumped Hydro	3.6	/

[a] The fuel efficiency is converted to Standard Coal Equivalent (SCE)/kWh.
[b] For gas fired units, we use the national average efficiency for power generation of 35%.

pattern as in 2018, increased proportionally according to total electricity demand. The interregional ultra-high voltage (UHV) transmission lines in WIM are assumed to expand to a capacity of 35 GW by 2030 [45].

The heating season in the WIM region covers approximately 180 days in winter. Hourly space heating demand is estimated by the indoor (18 °C) and outdoor temperature difference according to the hourly ambient temperature in 2018 taken from the NASA assimilated meteorological database, GEOS-5. The total space heating demand amounted to 59 TWh in 2018 and is projected to grow to 89 TWh assuming an annual growth rate of 3.5% based on historical data in Ref. [46]. Hourly variations of heat demand with time in 2030 are assumed to follow the pattern observed in 2018.

The wind data are derived from the optimal wind fields in the WIM area as compiled in the Modern-Era Retrospective analysis for Research and Applications (MERRA-2) of GEOS. Winds included in this dataset were obtained by retrospective analysis of global meteorological data using a state-of-the-art weather/climate model incorporating a variety of observational inputs from surface stations, aircraft, balloons, ships, buoys, dropsondes, and satellites. Based on the vertical profile of wind power introduced in Ref. [47], wind speeds at 100 m height are extrapolated from those at 50 m. Hourly wind power is then calculated using the power curve for a typical deployed onshore system, GE 2.5 MW wind turbines [48]. The installed wind capacity reached 18.2 GW in this area in 2018; in this study, we consider investments in additional wind adding up to as much as 100 GW in 2030. Fig. 3 illustrates the hourly power load, heat demand and wind power generation in 2018.

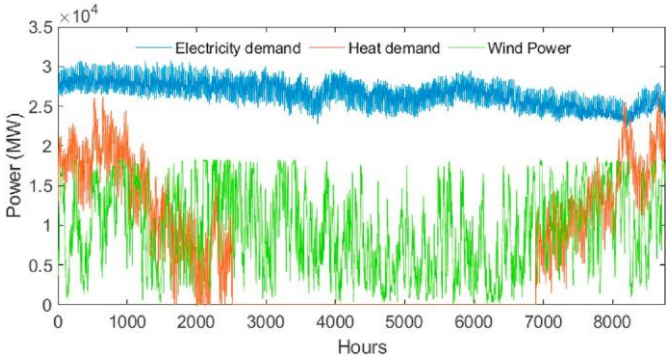

Fig. 3. Hourly electricity demand, heat demand, and wind supply in 2018.

2.2.2. Annual H_2 demand and CO_2 emission assumptions

Today, the bulk of the hydrogen produced from fossil fuels is used primarily in the manufacture of ammonia and methanol and in refining of petroleum. Hydrogen demand for the WIM area is estimated from the China Statistical Yearbook 2018 taking account of the annual production of ammonia and methanol and processing of crude oil. Adopted from Ref. [49], the hydrogen consumption for different industries and the weighting factors for production from fossil fuels are illustrated in Table 2.

Table 2
Industrial H_2 production information adopted from Ref. [49].

Industry	H_2 demand (kg/ton)	Weight factor for H_2 production (%)		
		Coal	Natural gas	Oil
Ammonia	180.31	64	23	13
Methanol	134.36	77	11	12
Oil Refinery	4.48	0	39	71
Chlor-alkali	24.9	/	/	/
Coke	21.4	/	/	/

Hydrogen can be generated also as a by-product of other manufacturing processes, extracted from industrial hydrogenous off-gases. Hydrogen produced from chlor-alkali and coke production are included in Table 2, expressed as negative values.

Based on [32], the national hydrogen demand for the chemical industry in 2030 is likely to increase by 19.1% compared to 2018 while a 10 million ton increment is projected for the iron and steel industry. The increase in WIM's industrial requirements for hydrogen in 2030 is calculated then on the basis of the chemical industry demand accounting additionally for the anticipated regional investments in iron and steel. The equations for calculating annual hydrogen demand, H_{total}, and the corresponding CO_2 emissions, E_{total}, are given as:

$$\begin{cases} H_{total} = \sum_{x=AMO}^{COK} d_x O_x \\ E_{total} = \sum_{oil}^{x=AMO} \sum_{x=AMO}^{COK} d_x O_x u_y ef_y \end{cases} \quad (1)$$

$$x = [AMO; MET; OIR; CHA; COK]$$
$$y = [coa; ng; oil]$$

where O_x and d_x represent the annual production and corresponding unit hydrogen demand for the industry of ammonia (x = AMO), methanol (x = MET), oil refinery (x = OIR), chlor-alkali (x = CHA) and coke (x = COK); u_y and ef_y indicate the weight factor for hydrogen produced from coal (y = coa), natural gas (y = ng) and oil (y = oil) in different industries and the emission factors for the sources.

The CO_2 emission factors for H_2 produced from coal, natural gas and oil without CCS are taken as 21.82, 13.24 and 13.8 ton of CO_2 per ton of H_2 respectively [33]. The emission factors for coal gasification and SMR with CCS and P2H from wind power are 5.61, 6.2 and 0.88 kg CO_2/kg H_2.

2.3. Hydrogen production with electrolysis technologies

Three types of electrolyzer cells are considered in this study: alkaline (AEC), proton exchange membrane (PEMEC) and solid oxide (SOEC) devices. AEC is currently the most mature and durable technology. It features low capital cost and high reliability but relatively low efficiency. It is also comparatively inflexible as a consequence of relatively long times for ramping and start-up. PEMEC offers higher power density and reactant rates and is capable also of producing compressed gases (>100 bar) available for direct storage without need for compressors. However, this technology requires expensive membranes and platinum catalysts. The SOEC option employs a solid oxide fuel cell running in reverse mode. With extra heat input and an associated increase in working temperature, the conversion efficiency for SOEC is significantly higher than the efficiency for the alternatives. Although experience to date is relatively limited compared with AEC, SOEC is considered the most promising future technology option for electrolysis [50].

2.3.1. Economic and technical characteristics of electrolysis technologies

The techno-economic data for the three electrolyzers are summarized in Table 3. Capital costs for the different systems include the electrolyzer, foundation, "turn-key" installation and all necessary auxiliary components such as feed water treatment, and systems for cooling and hydrogen purification (>99.99% for hydrogen). Annual fixed O&M expense is represented by the sum of maintenance, stack replacement and labor costs. Here, we focus only on the production process of green hydrogen for potential industrial utilization. The storage, compression and delivery costs associated with centralized and distributed hydrogen production for different application pathways will be analyzed in a further study.

Table 3
Techno-economic data of different electrolysis technologies [50e52].

	AEC		PEMEC		SOEC	
	2020	2030	2020	2030	2020	2030
Capital cost ($/kW)	692	604	1208	659	2415	659
Fixed O&M cost ($/kW/year)	33	30	61	33	72	20
Rated system efficiency (LHV)	61%	63%	58%	62%	76%	79%
Partial load range	20%e100%		5%e100%		0e100%	
System lifetime (years)	25		15		20	

Since one of our model assumptions is that the electrolyzer would produce hydrogen solely using variable wind power, it is necessary to determine the implications of the partial-load operation and the system power-to-hydrogen (P2H) efficiency considering auxiliary power consumption and efficiency degradation. The system P2H efficiency, the ratio between the lower heat value (LHV) of output hydrogen and the input power of the system, is calculated as:

$$e_{ec} = \frac{P_s(e_s - e_d)}{\frac{P_s}{e_c} + P_a + P_h} \times 100\% \quad (2)$$

where P_s and e_s represent the power and efficiency of the electrolyzer stack; e_d denotes the average lifetime degradation of the stack, summarized in Table 3; e_c is the efficiency of the AC/DC converter; P_a and P_h indicate the power consumption of the auxiliary equipment and the heat input, respectively.

The heat input for AEC and PEMEC technologies is assumed to be zero while that for SOEC is taken as 15% of the total energy input to the system [50]. Based on the statistics in Ref. [53], we assume that stack degradation leads to a lifetime average system efficiency 4% below the efficiency at the start of life. To define system efficiency profiles for the different electrolyzers, we assumed that the efficiency experience from real-world projects [54e56] could be scaled up considering the rated efficiencies given in Table 3 as well as the average degradation. Fig. 4 indicates the system P2H efficiency profiles for the different electrolysis systems in 2020.

2.3.2. Electrolysis hydrogen production optimization (EHPO) model

The EHPO was formulated to include the capacity design of the P2H system and to describe its economic operation on an hourly basis. The input includes hourly curtailed wind power, hourly on-grid wind power, technical and economic parameters for electrolysis technology and selected operation modes and orders for

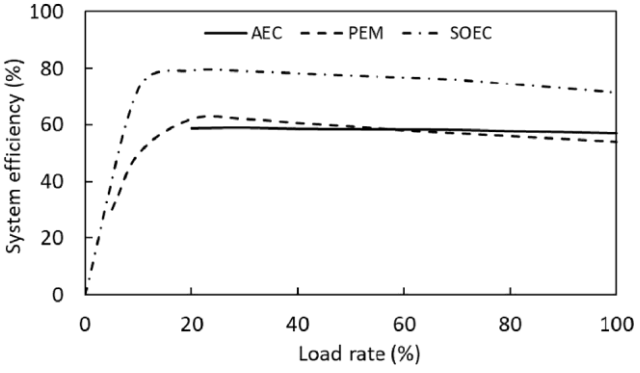

Fig. 4. Power-to-hydrogen efficiency profiles of different electrolysis system in 2020.

engagement of individual units. The output includes an optimal size for the P2H system components, hourly energy consumption and generation for each unit, and corresponding costs and revenues.

The decision variables include continuous specifications associated with system size and energy balance, binary variables associated with start-up states of individual units and Special-Ordered-Set (SOS) variables as weighting factors in linearization. The capacity of the electrolysis system is optimized based on wind investment to produce hydrogen at a cost lower than the marginal cost for fossil fuel-based production. The objective function is defined to minimize the overall system cost under the constraint of a specified production quota or to maximize the hydrogen output subject to a defined levelized cost of hydrogen (LCOH) constraint. The total cost (C_{total}) accounts for the amortized system capital cost (C_{cap}), the fixed O&M cost (C_{om}), and the annual operational cost (C_{op}):

Objective 1:

$$\min C_{total} = C_{cap} + C_{om} + C_{op} \tag{3}$$

such that:

$$\begin{cases} C_{cap} = I_{ec} \cdot \dfrac{a_{ec}}{\sum_{j=1}^{T} \frac{1}{(1+i)^j}} \\ C_{om} = I_{ec} \cdot a_{ec} \cdot b_{ec} \\ C_{op} = C_g + C_w - R_o - R_h \end{cases} \tag{4}$$

$$\begin{cases} I_{ec} = \sum_{n=1}^{N} I_{ec;n} \\ C_g = \sum_{n=1}^{N} \sum_{t=1}^{8760} P_{gw;t;n} \cdot p_g \\ C_w = \sum_{n=1}^{N} \sum_{t=1}^{8760} H_{t;n} \cdot g_w \cdot p_w \\ R_o = \sum_{n=1}^{N} \sum_{t=1}^{8760} H_{t;n} \cdot g_o \cdot p_o \\ R_h = \sum_{n=1}^{N} \sum_{t=1}^{8760} H_{t;n} \cdot g_h \cdot p_h \end{cases} \tag{5}$$

where I_{ec}, a_{ec}, b_{ec}, and T denote the installed capacity, capital cost, fixed O&M cost fraction and the lifetime for electrolysis system; i is the discount rate; C_g *and* C_w indicate the costs for purchasing grid electricity and water; R_o *and* R_{heat} represent the revenues realized by selling oxygen and heat; $I_{ec;n}$ is the capacity of the nth unit; $P_{gw;t;n}$ and $H_{t;n}$ denote the purchased on-grid wind power and hydrogen output of the nth unit at time t; g_w; g_o *and* g_h represent the water demand, oxygen output and heat output associated with unit hydrogen production and p_g; p_w; p_o *and* p_h indicate the unit prices for on-grid wind electricity, water, oxygen and heat, respectively.

Constraints including energy conversion and operation-related piecewise linearization, wind source capacity, operation mode, unit boot order and limitations for wind utilization and hydrogen output are considered in the model. The energy conversion during P2H process is expressed as:

$$H_{t;n} = e_{ec;t;n} \cdot \left(P_{cw;t;n} + P_{gw;t;n}\right) \tag{6}$$

$$0 \le P_{cw;t;n} + P_{gw;t;n} \le I_{ec;n} \tag{7}$$

where $P_{cw;t;n}$ represents the curtailed wind power input into the nth unit at time t, and $e_{ec;t;n}$ is the P2H efficiency of the nth electrolysis unit at time t.

In order to optimize the capacity of the P2H system, the P2H efficiency at full load level, e_{full}, is taken for the hourly basis operation at first. After the capacity is determined, a detailed operational optimization considering range limitation, partial loads and unit boot order are conducted to find the least cost for hydrogen production. This procedure helps to remain the liner of the model with SOS2 variables. Traditional bilevel programming, heuristic method and the Karush–Kuhn–Tucker (KKT) conditions are also commonly used for this type of mathematical problem but faced with unique drawbacks. For capacity optimization, Equation (6) is transferred to:

$$H_{t;n} = e_{full} \cdot \left(P_{cw;t;n} + P_{gw;t;n}\right) \tag{8}$$

$$e_{full} = e_{rate} - e_d \tag{9}$$

For operational optimization, the nonlinear efficiency functions (Fig. 4) are expressed by piece-wise linear approximations based on SOS2 variables. Equation (6) is replaced by the following constraints:

$$e_{ec;t;n} = e_{ec;k} \cdot x_{k;t;n} \tag{10}$$

$$P_{w;t;n} + P_{g;t;n} = I_{ec;n} \cdot \sum_{k}^{K} I_{ec;k} \cdot x_{k;t;n} \tag{11}$$

$$H_{t;n} = I_{ec;n} \cdot \sum_{k}^{K} I_{ec;k} \cdot e_{ec;k} \cdot x_{k;t;n} \tag{12}$$

where $e_{ec;k}$ and $I_{ec;k}$ indicate the set of discrete efficiency and load levels at the kth point; $x_{k;t;n}$ are the weighting variables contained in a SOS2 set, in which no more than two consecutive elements can be non-zero. The related constraints are:

$$x_{k;t;n} \ge 0 \tag{13}$$

$$\sum_{k}^{K} x_{k;t;n} = bin_{t;n} \text{ and } x_{k;t;n} + x_{k-1;t;n} \ge 0 \text{ for up to two elements (SOS2)} \tag{14}$$

where $bin_{t;n}$ indicates the on/off status of the electrolysis unit.

The introduce of binary variables ensures that the input power of the P2H system satisfies its performance constraints while the lower bond is not zero, like the AEC system. For operational optimization, Equation (7) is reconstructed as:

$$bin_{t;n} \cdot I_{ec;n} \cdot U_{;1} \le P_{w;t;n} + P_{g;t;n} \le bin_{t;n} \cdot I_{ec;n} \cdot U_{;K} \tag{15}$$

The integration of curtailed and on-grid wind power are constrained by the total capacity, associated with the hourly capacity factor calculated based on the physical potential and the operation of the grid system:

$$P_{cw;t;n} \ge 0 \tag{16}$$

$$P_{gw;t;n} \geq 0 \tag{17}$$

$$\sum_{n=1}^{N} \sum_{t=1}^{8760} P_{cw;t;n} \leq P_{cw;t} \tag{18}$$

$$\sum_{n=1}^{N} \sum_{t=1}^{8760} P_{gc;t;n} \leq P_{gw;t} \tag{19}$$

Two operation modes are considered for the P2H system, the default setting represents the mode that uses both curtailed and on-grid wind power. The constraint for the operation mode where we use only curtailed wind power is:

$$P_{g;t;n} = 0 \tag{20}$$

When multiple electrolysis units are operated simultaneously, the operation order of different units needs to be fixed. Operating synchronously means equal output from multiple sources at the same time, while operating asynchronously means that only one device is permitted to run when the load is less than its rated capacity and the remaining devices are allowed to start one-by-one when the load exceeds the rated capacity of an individual device. In our calculation, operating synchronously is considered the default situation. The constraint for operating synchronously is expressed as:

$$x_{k;t;1} = x_{k;t;2} = \ldots = x_{k;t;N} \tag{21}$$

The constraint for operating asynchronously is expressed as:

$$x_{K;t;n} \geq \sum_{k} x_{k;t;n-1} = bin_{t;n-1} \tag{22}$$

Two additional constraints are added for objective function 1 according to the calculation scenario: constraint (22) is considered to achieve an expected level of curtailed wind utilization and constraint (22) represents the requirement that the annual hydrogen production should meet the annual demand:

$$\sum_{n=1}^{N} \sum_{t=1}^{8760} P_{cw;t;n} \geq f \cdot \sum_{t=1}^{8760} P_{cw;t} \tag{23}$$

$$\sum_{n=1}^{N} \sum_{t=1}^{8760} H_{t;n} \geq H_{total} \tag{24}$$

where f indicates the utilization rate of curtailed wind and H_{total} defines the annual hydrogen demand.

To maximize the hydrogen output amount under a LCOH constraint, the objective function is:

Objective 2:

$$\max A_{hyd} = \sum_{n=1}^{N} \sum_{t=1}^{8760} h_{sys;t;n} \cdot \left(P_{w;t;n} - P_{g;t;n}\right) \tag{25}$$

Subject to

$$C_H \cdot H_{total} \leq C_{cap} - C_{om} - C_{op} \tag{26}$$

Constraints (4)e(22) remain unchanged for objective function (25).

The value of the parameters for the EHPO model in the present study are summarized in Table 4. Instead of taking the lower levelized cost of wind power, the adopted on-grid wind electricity price, also called the feed-in tariff, guarantees that the income from the installed wind turbines/plants will not decline when integrated with additional hydrogen production. It should be noted that the revenue that could be realized by selling heat from different electrolysis systems is not included in the optimization due to lack of data on potential applications. However, in response to anticipated continuous improvements of the auxiliary facilities in electrolysis systems, utilization of the heat output should contribute to a reduction in demands for operation of CHP units improving thus enhance the flexibility of the grid.

3. Results and discussion

This section summarizes the results for the energy system simulation and the costs and outputs identified for corresponding hydrogen production.

3.1. General results of wind power in WIM

Power systems for WIM are simulated on an hourly basis throughout a year for a range of wind investment levels. The variation of daily wind power output and curtailment at three representative wind installed capacities are illustrated in Fig. 5. The results indicate that the curtailment rate is much higher during the winter season. The curtailment rates increase significantly with the rise of wind penetration levels. With an increased electricity demand and the planned expansion of the UHV network, the curtailment rate in 2030 corresponding to a 50 GW wind installation is 8.1%, lower than in 2018 (10.2%) in this area despite the much larger capacity for installed wind systems assumed for 2030. Were the wind investment level to reach 100 GW, the curtailment rate would increase to 42.8%.

3.2. Hydrogen production cost under different levels of wind investment

The levelized production costs of hydrogen (LCOH) with only curtailed wind power (a) and with curtailed and on-grid wind power (b) for the three types of P2H electrolyzers are illustrated in Fig. 6. The cost efficiency of the electrolysis technology in 2030 is calculated based on a 10% curtailed wind utilization rate in Fig. 6 (a). Producing enough hydrogen to meet the industrial demand (950 kT/year) in WIM is set as the constraint in Fig. 6 (b) for operation with curtailed and on-grid wind power. It is shown that the H_2 production cost decreases with the increase in installed wind power capacity. This is as expected since more wind power will be curtailed as a result of the increase in installed wind power capacity.

For this study, the electrolysis system works in two modes. When operating with only curtailed wind power, the H_2 cost is very high with a wind system capacity lower than 30 GW (curtailment rate < 0.5%) since the available curtailed wind power for producing H_2 is relatively minor. In the operation mode including on-grid

Table 4
Value of the parameters for the EHPO model in the present study.

Parameter	Value	Ref
Oxygen price	0.04 $/kg	[57]
Water price	0.01 $/kg	[58]
On-grid wind electricity price	0.041 $/kWh	[59]
Discount rate	5%	
LHV of hydrogen	33.3 kWh/kg	[60]
Water consumption	9 kg/kg H_2 production	
Oxygen output	8 kg/kg H_2 production	

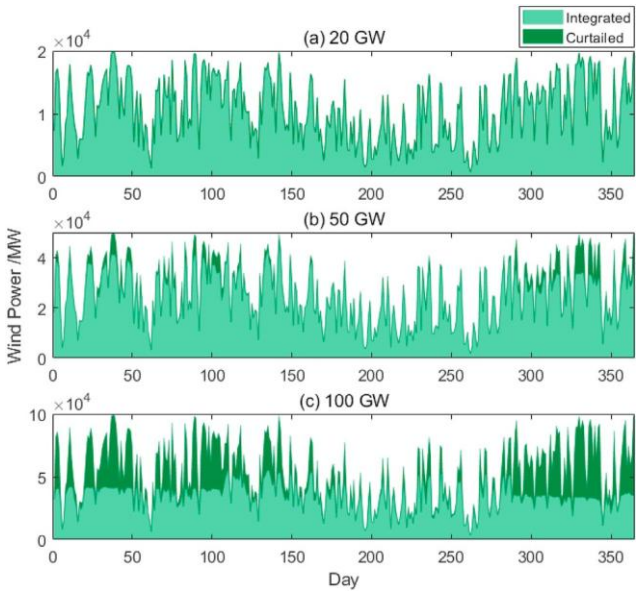

Fig. 5. Daily variation of wind power across the whole year in 2030.

wind power, the electrolysis plant operates with an optimal combination of curtailed and on-grid wind power to meet the industrial demand in WIM. The feed-in tariff for wind electricity in WIM, 0.041 $/kWh, is taken as the cost for using on-grid wind power [35]. It is shown that operation with curtailed wind is more cost effective if wind power capacity exceeds 50 GW (curtailment rate > 8.1%). This reflects the fact that for this case it is assumed that the cost for power that would otherwise be curtailed is essentially zero.

With respect to the three P2H technologies considered, SOEC is identified as the most cost-effective option for 2030. The target LCOH (2 $/kg) with central electrolysis identified as a target by the U.S. Department of Energy [19] (red dashed line) is used as a benchmark to demonstrate the economic feasibility of using P2H technology. The results indicate that P2H with SOEC can be economically viable if the wind power investments exceed 40 GW (curtailment rates > 3%). When the wind curtailment rate is larger than 14%, all three types of electrolysis systems can be cost-competitive regardless of operation mode.

3.2.1. Impacts of curtailed wind utilization, system degradation and cost uncertainty

The simulated 50 GW wind investment scenario (with a curtailment rate of 8.1%) can represent the current situation in WIM, in which wind curtailment reached 9% in 2019. 50 GW of wind capacity is therefore taken as a typical scenario for the following analysis.

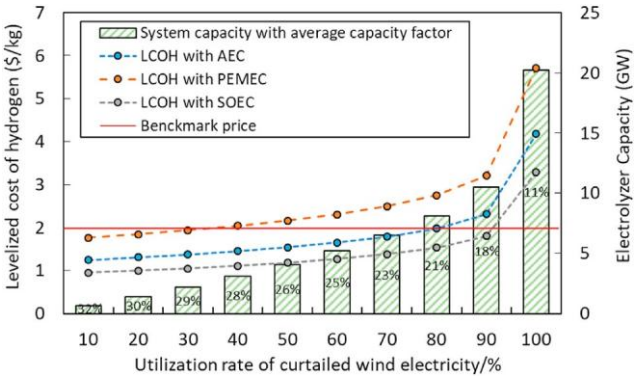

Fig. 7. Hydrogen production with only curtailed wind power in 2030.

The levelized production costs of hydrogen (LCOH) with only curtailed wind power for the three types of P2H electrolyzers are illustrated in Fig. 7. It is shown that the LCOH increases with the increase of curtailed wind utilization. The reason for this is that a larger capacity of electrolysis systems must be installed to meet larger peak availability of curtailed wind. This phenomenon becomes more obvious at higher level of wind utilization. To meet the highest peaks, all the LCOH of the three P2H technologies increase dramatically when the utilization rate of curtailed wind electricity rises from 90% to 100%. As shown with the bar chart in Fig. 7, the average capacity factor (CF) for the electrolysis system decreases when using a larger proportion of curtailed wind. The equipment investment represents the bulk of the overall cost for the systems deployed to produce H_2 when only curtailed wind is used: a higher CF results in a lower LCOH. The results here indicate the importance and necessity of integrating renewable power flow into P2H system optimization. The capacity design for water electrolysis should be matched with wind capacity and power curtailment. Otherwise, it will not be possible to achieve the goal for efficient utilization of renewable power while at the same time improving economic benefits.

Data from academic literature [19,53,61] and reports [50,51] indicate significant uncertainty in the development of P2H technologies with respect to future cost, efficiency and lifetime. In order to explore the impact of potential future advances in electrolysis technologies on costs of H_2 production from wind power, the techno-economic data for 2020 and 2030 presented in Table 3 are taken as the boundary assumptions to determine the range of

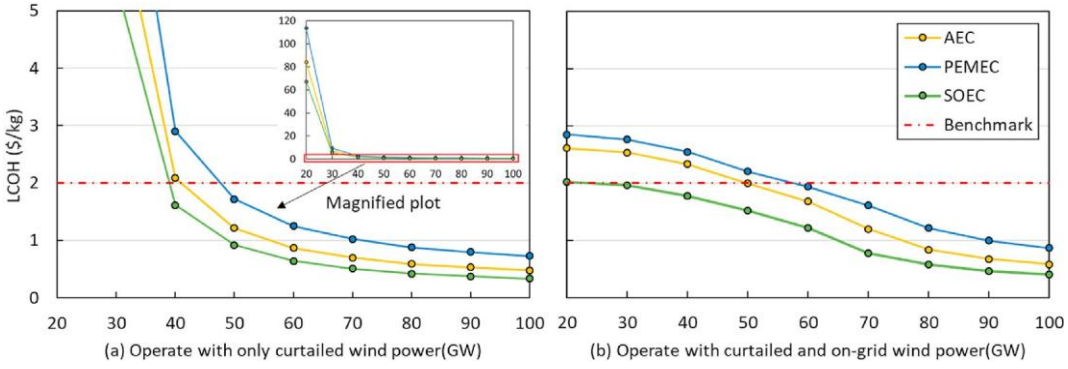

Fig. 6. Levelized hydrogen production cost under different wind power capacity in 2030.

LCOH. The technological uncertainty considered in this study is consistent with the projections by experts in Ref. [61] with respect to opportunities for production scale-up in response to anticipated different levels of future funding for research and development. The system degradation and lifetime effect are further investigated by an operational lifetime estimation scenario (OLTS), where the lifetime given in Table 3 is adopted as the operational lifetime for the electrolysis system. This assumption is based on the fact that electrolyzers do not require a protective current in stand-by mode and that stack degradation is commonly assessed in terms of operation time [53,54]. The amortized system capital cost calculation is reconstructed as equation (27) for the OLTS. The effects of transient operation on stack and system lifetime are not yet well quantified, but the proposed framework provides a ready means to integrate information on degradation mechanisms if and when it should become available.

$$C_{cap} = I_{ec} \cdot \frac{a_{ec}}{\sum_{j=1}^{T} \frac{1}{(1+i)^j}} \cdot \frac{\sum_{n=1}^{N} \sum_{t=1}^{8760} bin_{t,n}}{8760 \cdot N} \quad (27)$$

The range of LCOH considering only curtailed wind power is illustrated in Fig. 8 for the three different options for P2H technology. It is shown that the SOEC technology has the largest range of cost variation over the coming decade, indicating a relatively high P2H efficiency together with a relatively high potential to reduce capital costs with production scale-up after commercialization. In contrast, the AEC technology has a much smaller change in LCOH due to comparatively mature stack components and the avoidance of noble metals in manufacturing. We shall argue that AEC would be more suitable in 2020 under the current market production situation, but this situation is likely to change in favor of SOEC in the future. The green line in Fig. 8 illustrates the H_2 production cost that excludes the cost for degradation when the electrolysis system is not in use. It is shown that the LCOH could reach 0.5 $/kg if operational time is taken to define its lifetime. This follows straightforwardly since wind power curtailment happens only occasionally, extending therefore the overall existing lifetime of P2H plants under OLTS.

3.2.2. Comparison of hydrogen output with respect to operational mode and cost

For this study, the electrolysis system operates in two possible modes, i.e., with and without on-grid wind power. As the most cost-effective option for 2030, the performance of SOEC under different operational modes illustrates their effects.

The SOEC system performance under the two operational modes is compared in Fig. 9. It is shown that the integration of on-grid power significantly enhances the production of H_2 without an increase in LCOH. In other words, with a sufficient amount of on-grid power integration, the electrolysis system could produce a larger amount of H_2 at a lower LCOH. This may seem surprising since the purchase of on-grid wind power adds to the system's economic burden especially when the source from curtailed wind is assumed to be free. The results in Fig. 9 (b) and (c) provide an explanation. They show that, with on-grid wind power, electrolysis has a smaller system capacity requirement at LCOH levels above 1.5 $/kg and a much higher average system CF compared to the mode with only curtailed wind, which indicates a positive return on investment (ROI) when producing an additional unit of H_2 with purchased electricity. However, Fig. 9 (d) shows that operating with curtailed wind power is the best way to achieve a very low LCOH, 1 $/kg for example, but the consequence is a relatively small output of hydrogen. In Fig. 9 (c), the average CF of the electrolysis system peaked at an LCOH of 1.5 $/kg because of the volatility of wind power generation and the operating rule that only wind power can be used to produce hydrogen. It indicates that the bulk of hourly wind power is larger than the capacity value of the electrolysis system to produce hydrogen at 1.5 $/kg. When the capacity of the system increases further, the CF will drop because the wind power at some hours of the year is not large enough to maximize the output.

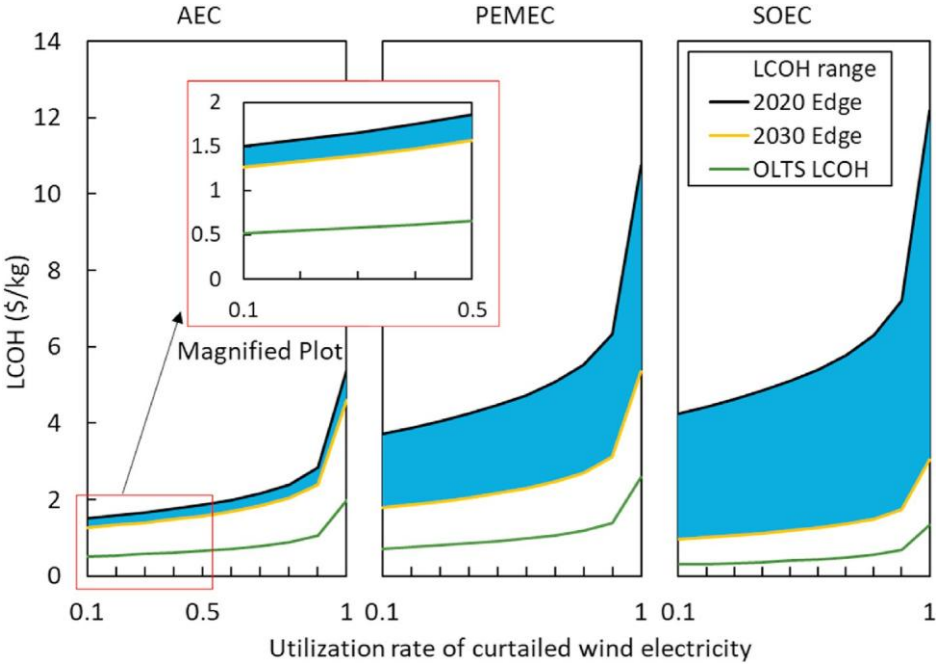

Fig. 8. Hydrogen production cost range.

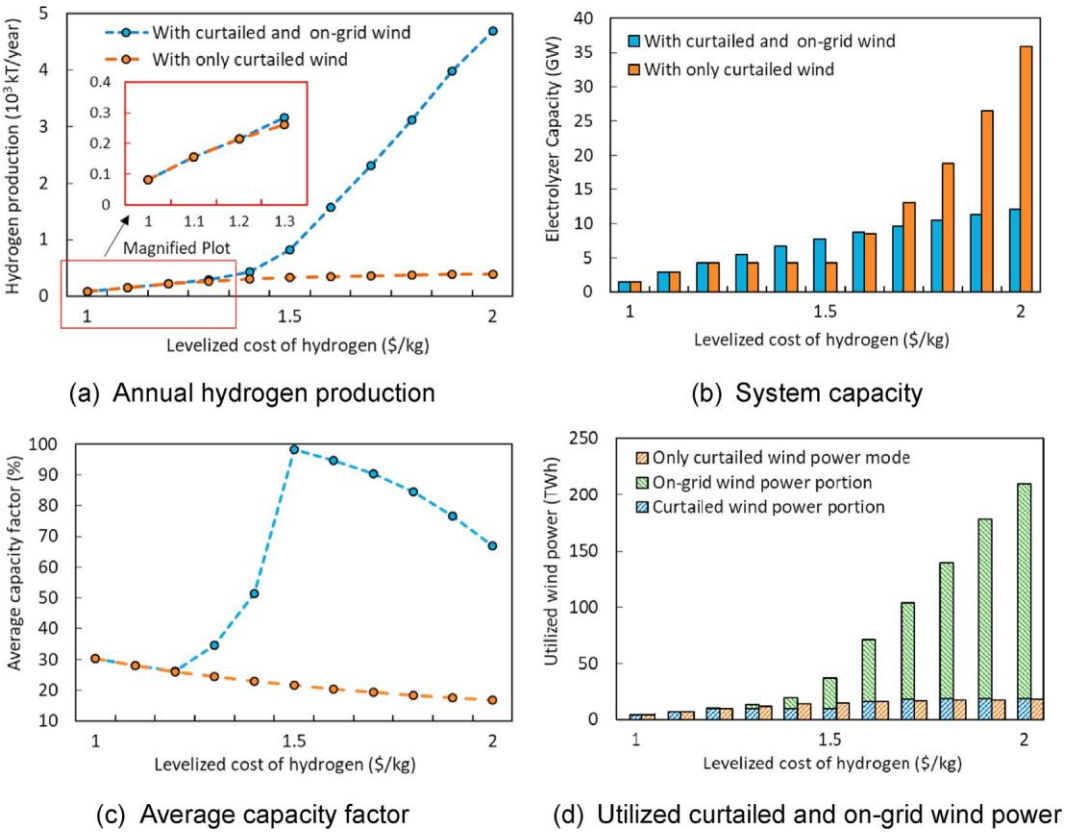

Fig. 9. Hydrogen production with SOEC at different cost.

3.3. *Impacts on hydrogen supply and CO_2 reduction*

The hydrogen production data in section 3.2.2 were selected to evaluate the impacts of P2H on hydrogen supply and CO_2 reduction. The industrial hydrogen demand was 1665.76 kT in 2018 in Inner Mongolia based on the calculation method described in section 2.3.3. Considering by-product H_2 totaling 602.88 kT from coke production and 74.04 kT from chlor-alkali production, the net demand is 988.84 kT for Inner Mongolia and 692.19 kT for WIM according to the regional GDP distribution. The projected net industrial H_2 demand amounts to 950 kT/year for WIM in 2030.

From Fig. 10, the hydrogen produced with only curtailed wind power could meet the industrial demand in WIM when the wind system capacity exceeds 60 GW. At a 50 GW wind investment level, the amount of hydrogen produced with curtailed wind could satisfy about 40% of net industrial demand. The hydrogen produced with curtailed wind at lower levels is significantly less than required to support the regional demand. However, thanks to the high P2H efficiency, the SOEC technology is capable of producing cost-effective H2 using on-grid wind power if the curtailed wind source is insufficient. At an LCOH of 1.52 $/kg, the H_2 produced could meet all the industrial demand in WIM. Up to 500% of the industrial demand in WIM can be met at a cost of less than 2 $/kg, approximately 13% of the projected national Chinese demand for H_2 in 2030 [32].

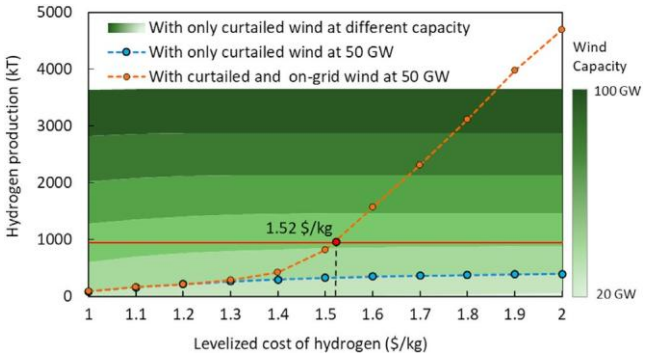

Fig. 10. Hydrogen demand satisfied with SOEC technology.

The maximum amount of hydrogen that could be produced at a cost lower than 2 $/kg and the corresponding CO_2 emission reductions with SOEC technology are summarized in Fig. 11. Based on the current generation mix of fossil-fuel based H_2, the reduction in CO_2 emissions would amount to 18.87 tons per year associated with every ton of green H_2 production in WIM. Even if CCS is fully utilized, every ton of green hydrogen produced from wind could still reduce annual carbon emissions by as much as 6.16 tons. Given the fact that no CCS for hydrogen production is currently available in China, the results indicate that P2H technology could contribute to a reduction of more than 200 million tons of CO_2 emissions per year with a 100 GW wind system investment, approximately the annual carbon footprint of Beijing [62]. It is noted that the carbon emissions of the grid power are not considered in the calculation since it is assumed that the purchased on-grid wind power would be supplied by newly installed wind capacity, without influencing grid operations and wind farm economics.

4. Conclusion

This study reports an integrated analysis for the economic feasibility and decarbonization potential of green hydrogen production in China's Western Inner Mongolia (WIM). The analysis

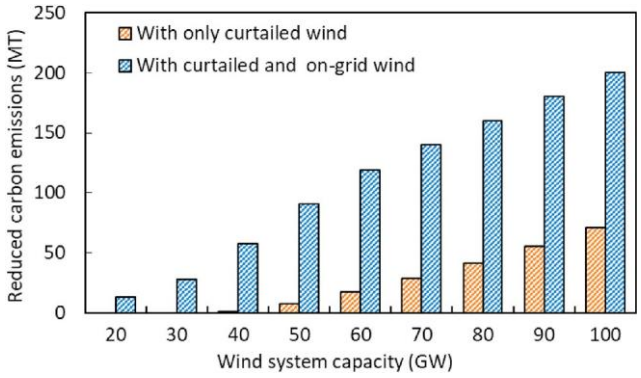

Fig. 11. Reduced carbon emissions with SOEC technology, compared to fossil fuel-based hydrogen production without CCS.

framework incorporates actual power demand, assimilated wind speed data, power system operations and diverse electrolysis system planning. From the technology viewpoint, alkaline electrolyzers (AEC) and solid oxide electrolyzers (SOEC) are identified as the most cost-effective technological options for 2020 and 2030, respectively. In the simulated 50 GW wind investment scenario (with a curtailment rate of 8.1%), all of the industrial demand for hydrogen in WIM (950 kT/year) could be met by production from power generated from wind at a cost of 1.52 $/kg. Facing frequent start-ups and shutdowns, the levelized cost of hydrogen (LCOH) drops to 0.5 $/kg with the duty cycle of electrolysis considered when calculating the lifetime. Here, we focus only on the production process of green hydrogen. Future studies will consider both storage and delivery costs for hydrogen distribution.

From the policy perspective, our findings could serve as a reference for the necessity for adjustments in the subsidies for renewable energy. Currently, renewable energy can earn a subsidy only when integrated into the grid. Policymakers could lend support specifically for hydrogen investments to accelerate large scale development and to lower the financial risks associated with renewable power investment.

China, as the world's largest emitter of greenhouse gases, responsible at the same time for the world's largest commitment to wind power, is facing dual challenges not only to mitigate its emissions but also to reduce the financial burden associated with excessive curtailment of its wind resources. Hydrogen is an ideal clean energy carrier with multiple applications not only for industry but also for transportation. This study provides evidence for both the sustainability and affordability of green hydrogen production addressing at the same time the challenges associated with the intermittency problems endemic to renewable power. As indicated, a significant portion of green hydrogen produced from wind power could be available at costs competitive with current production from fossil fuels. The analytical methods and lessons developed here for China should be applicable also to other countries, to Australia and Demark for example, where green hydrogen is currently benefiting from strong public support.

CRediT authorship contribution statement

Haiyang Lin: Conceptualization, Methodology, Software, Formal analysis, Writing – original draft, Writing – review & editing. Qiuwei Wu: Conceptualization, Investigation, Resources, Data curation. Xinyu Chen: Conceptualization, Methodology, Software, Formal analysis, Writing – original draft, Writing – review & editing, Supervision. Xi Yang: Investigation, Formal analysis, Writing – review & editing. Xinyang Guo: Resources, Methodology, Software. Jiajun Lv: Resources, Methodology, Software. Tianguang Lu: Investigation, Resources, Methodology, Formal analysis, Writing – review & editing. Shaojie Song: Investigation, Formal analysis, Writing – review & editing. Michael McElroy: Conceptualization, Methodology, Investigation, Writing – review & editing, Supervision, Project administration.

Declaration of competing interest

The authors declare that they have no known competing financial interests or personal relationships that could have appeared to influence the work reported in this paper.

Acknowledgements

This work was supported by the program for Outstanding PhD candidate of Shandong University, the scholarship from China Scholarship Council and the program titled "China 2030/2050: Energy and Environmental Challenges for the Future" from the Harvard Global Institute and the Energy Foundation China (G-2008-32164). The authors would also like to acknowledge instructive contributions from Chris P. Nielsen.

References

[1] IRENA, Renewable Capacity Statistics 2020, International Renewable Energy Agency (IRENA), Abu Dhabi, 2020.
[2] X. Han, X. Chen, M.B. McElroy, S. Liao, C.P. Nielsen, J. Wen, Modeling formulation and validation for accelerated simulation and flexibility assessment on large scale power systems under higher renewable penetrations, ApEn 237 (2019) 145–154.
[3] Grid Connection of Onshore Wind Power in 2019, National Energy Administration, 2020.
[4] X. Chen, M.B. McElroy, Q. Wu, Y. Shu, Y. Xue, Transition towards higher penetration of renewables: an overview of interlinked technical, environmental and socio-economic challenges, Journal of Modern Power Systems and Clean Energy 7 (2019) 1–8.
[5] G. Luo, E. Dan, X. Zhang, Y. Guo, Why the wind curtailment of northwest China remains high, Sustainability 10 (2018) 570.
[6] Q. Ye, L. Jiaqi, Z. Mengye, Wind curtailment in China and lessons from the United States, 2018. Brookings China's Energy in Transition Series.
[7] P. Larscheid, L. Lück, A. Moser, Potential of new business models for grid integrated water electrolysis, Renew. Energy 125 (2018) 599–608.
[8] T. Skoczkowski, E. Verdolini, S. Bielecki, M. Kochan‚ski, K. Korczak, A. We¸glarz, Technology innovation system analysis of decarbonisation options in the EU steel industry, Energy 212 (2020) 118688.
[9] IEA, The Future of Hydrogen, IEA, Paris, 2019. https://www.iea.org/reports/the-future-of-hydrogen.
[10] S. Mohanty, S. Lewis, F. Wang, China Ponders Subsidies, Cheaper Technology for its Hydrogen Roadmap, S&P Global Platts, Singapore, 2020.
[11] M. Deymi-Dashtebayaz, A. Ebrahimi-Moghadam, S.I. Pishbin, M. Pourramezan, Investigating the effect of hydrogen injection on natural gas thermo-physical properties with various compositions, Energy 167 (2019) 235–245.
[12] J.J. Lo‚pez Cascales, M.C. Juan-Segovia, J. Iba‚n-ez Molina, J. Sa‚nchez Vera, P.M. Vivo Vivo, Environmental impact associated with the substitution of internal combustion vehicles by fuel cell vehicles refueled with hydrogen generated by electrolysis using the power grid. An estimation focused on the Autonomous Region of Murcia (Spain), Renew. Energy 77 (2015) 79–85.
[13] B.B. Ale, S.O. Bade Shrestha, Introduction of hydrogen vehicles in Kathmandu Valley: a clean and sustainable way of transportation, Renew. Energy 34 (2009) 1432–1437.
[14] M. Robinius, T. Raje, S. Nykamp, T. Rott, M. Müller, T. Grube, B. Katzenbach, S. Küppers, D. Stolten, Power-to-Gas: electrolyzers as an alternative to network expansion – an example from a distribution system operator, ApEn 210 (2018) 182–197.
[15] G. Squadrito, A. Nicita, G. Maggio, A size-dependent financial evaluation of green hydrogen-oxygen co-production, Renew. Energy 163 (2021) 2165–2177.
[16] H. Ishaq, I. Dincer, Comparative assessment of renewable energy-based hydrogen production methods, Renew. Sustain. Energy Rev. 135 (2021) 110192.
[17] S. Toghyani, E. Afshari, E. Baniasadi, M.S. Shadloo, Energy and exergy analyses of a nanofluid based solar cooling and hydrogen production combined system, Renew. Energy 141 (2019) 1013–1025.
[18] M.R. Shaner, H.A. Atwater, N.S. Lewis, E.W. McFarland, A comparative technoeconomic analysis of renewable hydrogen production using solar energy, Energy Environ. Sci. 9 (2016) 2354–2371.

[19] G. Glenk, S. Reichelstein, Economics of converting renewable power to hydrogen, Nat. Energy 4 (2019) 216e222.
[20] R.P. Micena, O.R. Llerena-Pizarro, T.M. de Souza, J.L. Silveira, Solar-powered hydrogen refueling stations: a techno-economic analysis, IJHE 45 (2020) 2308e2318.
[21] G. Zhang, J. Zhang, T. Xie, A solution to renewable hydrogen economy for fuel cell buses e a case study for Zhangjiakou in North China, IJHE 45 (2020) 14603e14613.
[22] E. Solomin, I. Kirpichnikova, R. Amerkhanov, D. Korobatov, M. Lutovats, A. Martyanov, Wind-hydrogen standalone uninterrupted power supply plant for all-climate application, IJHE 44 (2019) 3433e3449.
[23] H. Mehrjerdi, Peer-to-peer home energy management incorporating hydrogen storage system and solar generating units, Renew. Energy 156 (2020) 183e192.
[24] E.I. Koytsoumpa, S. Karellas, E. Kakaras, Modelling of Substitute Natural Gas production via combined gasification and power to fuel, Renew. Energy 135 (2019) 1354e1370.
[25] E. van der Roest, L. Snip, T. Fens, A. van Wijk, Introducing Power-to-H3: combining renewable electricity with heat, water and hydrogen production and storage in a neighbourhood, ApEn 257 (2020) 114024.
[26] E.F. Bødal, M. Korpås, Value of hydro power flexibility for hydrogen production in constrained transmission grids, IJHE 45 (2020) 1255e1266.
[27] O. Bamisile, J. Li, Q. Huang, S. Obiora, P. Ayambire, Z. Zhang, W. Hu, Environmental Impact of Hydrogen Production from Southwest China's Hydro Power Water Abandonment Control, IJHE, 2020.
[28] J. Kotowicz, D. We˛cel, M. Jurczyk, Analysis of component operation in power-to-gas-to-power installations, ApEn 216 (2018) 45e59.
[29] E. Frank, J. Gorre, F. Ruoss, M.J. Friedl, Calculation and analysis of efficiencies and annual performances of Power-to-Gas systems, ApEn 218 (2018) 217e231.
[30] J. Kotowicz, Ł. Bartela, D. W˛cel, K. Dubiel, Hydrogen generator characteristics for storage of renewably-generated energy, Energy 118 (2017) 156e171.
[31] Z. Mao, Z. Mao, The Hydrogen Production Process and Technology, Chemical Industry Press, 2018.
[32] C.H. Alliance, White Paper on Hydrogen Energy and Fuel Cell Industry in China, 2019.
[33] B. Parkinson, P. Balcombe, J.F. Speirs, A.D. Hawkes, K. Hellgardt, Levelized cost of CO2 mitigation from hydrogen production routes, Energy Environ. Sci. 12 (2019) 19e40.
[34] G. Pan, W. Gu, H. Qiu, Y. Lu, S. Zhou, Z. Wu, Bi-level mixed-integer planning for electricity-hydrogen integrated energy system considering levelized cost of hydrogen, ApEn 270 (2020) 115176.
[35] X.Y. Chen, M.B. McElroy, C.Q. Kang, Integrated energy systems for higher wind penetration in China: formulation, implementation, and impacts, IEEE Trans. Power Syst. 33 (2018) 1309e1319.
[36] X. Chen, H. Zhang, Z. Xu, C.P. Nielsen, M.B. McElroy, J. Lv, Impacts of fleet types and charging modes for electric vehicles on emissions under different penetrations of wind power, Nat. Energy 3 (2018) 413e421.
[37] N. Zhang, X. Lu, M.B. McElroy, C.P. Nielsen, X. Chen, Y. Deng, C. Kang, Reducing curtailment of wind electricity in China by employing electric boilers for heat and pumped hydro for energy storage, ApEn 184 (2016) 987e994.
[38] X. Chen, J. Lv, M.B. McElroy, X. Han, C.P. Nielsen, J. Wen, Power system capacity expansion under higher penetration of renewables considering flexibility constraints and low carbon policies, IEEE Trans. Power Syst. 33 (2018) 6240e6253.
[39] Grid Connection of Onshore Wind Power in 2018, National Energy Administration, 2019. http://www.nea.gov.cn/2019-01/28/c_137780779.htm.
[40] Grid Integration of Solar Power in 2018, National Energy Administration, 2019. http://www.nea.gov.cn/2019-03/19/c_137907428.htm.
[41] Global Energy Observatory. http://globalenergyobservatory.org/constructNetworkIndex.php.
[42] Almanac of China's water power. https://data.cnki.net/trade/Yearbook/Single/N2008030047?z¼Z025, 2017.
[43] Haiwang Zhong, Qing Xia, Yuguo Chen, Chongqing Kang, Energy-saving generation dispatch toward sustainable electric power industry, Energy Pol. 83 (2015) 14e25.
[44] S.G.E.R. Institute, Research on Electricity Demand Forecasting, State Grid Corporation of China, 2013.
[45] The Thirteenth Five Year Plan of Power Development for Inner Mongolia, State Development and Reform Commission of Inner Mongolia, Hohhot, China, 2017.
[46] Ministry of housing and urban-rural construction of China, China Urban Construction Statistical Year Book 2018, China Housing and Urban-Rural Construction Press, Beijing, China, 2018.
[47] C.L. Archer, M.Z. Jacobson, Evaluation of global wind power, J. Geophys. Res.: Atmosphere 110 (2005).
[48] X. Chen, X. Lu, M.B. McElroy, C.P. Nielsen, C. Kang, Synergies of wind power and electrified space heating: case study for Beijing, Environ. Sci. Technol. 48 (2014) 2016e2024.
[49] X. Deng, H. Wang, H. Huang, M. Ouyang, Hydrogen flow chart in China, IJHE 35 (2010) 6475e6481.
[50] Technology Data for Renewable Fuels, Danish Energy Agency, 2019.
[51] L. Bertuccioli, et al., Study on development of water electrolysis in the EU, 2014. Tech. Rep. February.
[52] M. Felgenhauer, T. Hamacher, State-of-the-art of commercial electrolyzers and on-site hydrogen generation for logistic vehicles in South Carolina, IJHE 40 (2015) 2084e2090.
[53] A. Buttler, H. Spliethoff, Current status of water electrolysis for energy storage, grid balancing and sector coupling via power-to-gas and power-to-liquids: a review, Renew. Sustain. Energy Rev. 82 (2018) 2440e2454.
[54] D. Scho€nberger, P2G durch Elektrolyse e eine flexible Speicherlo€sung, Zürich, 2016.
[55] Y. Lu, J. Li, L. Souamy, J. Wang, Y. Zhang, B. Zhu, Model Analysis on Hydrogen Production by Hybrid System of SOEC and Solar Energy, 2017.
[56] V.M. Nikolic, G.S. Tasic, A.D. Maksic, D.P. Saponjic, S.M. Miulovic, M.P. Marceta Kaninski, Raising efficiency of hydrogen generation from alkaline water electrolysis e energy saving, IJHE 35 (2010) 12369e12373.
[57] S. Alavandi, J. Seaba, G. Subbaraman, Emerging and Existing Oxygen Production Technology Scan and Evaluation, Gas Technology Institute, 2018.
[58] Y. Li, D.W. Chen, M. Liu, R.Z. Wang, Life cycle cost and sensitivity analysis of a hydrogen system using low-price electricity in China, IJHE 42 (2017) 1899e1911.
[59] Notice of the National Development and Reform Commission on Improving the On-Grid Tariff Policy for Wind Power, 2019.
[60] Energy Density of Hydrogen, The Physics Factbook, 2005.
[61] O. Schmidt, A. Gambhir, I. Staffell, A. Hawkes, J. Nelson, S. Few, Future cost and performance of water electrolysis: an expert elicitation study, IJHE 42 (2017) 30470e30492.
[62] Z. Liu, B. Cai, High-resolution Carbon Emissions Data for Chinese Cities, Environment and Natural Resources Program, Belfer Center, 2018. Available at, https://www.belfercenter.org/publication/high-resolution-carbon-emissions-datachinese-cities.